Published in final edited form as:

Brain Struct Funct. 2015 November ; 220(6): 3555–3564. doi:10.1007/s00429-014-0873-y.

Striatal GABA-MRS predicts response inhibition performance and its cortical electrophysiological correlates

Clara Quetscher[1,2], **Ali Yildiz**[2], **Shalmali Dharmadhikari**[3,4], **Benjamin Glaubitz**[5], **Tobias Schmidt-Wilcke**[5], **Ulrike Dydak**[3,4], and **Christian Beste**[1,2]

[1]Cognitive Neurophysiology, Department of Child and Adolescent Psychiatry, Faculty of Medicine of the TU Dresden, Germany

[2]Institute for Cognitive Neuroscience, Biopsychology, Ruhr-Universität Bochum, Germany

[3]School of Health Sciences, Purdue University, West Lafayette, USA

[4]Department of Radiology and Imaging Sciences, Indiana University School of Medicine, Indianapolis, USA

[5]Department of Neurology, Berufsgenossenschaftliche Kliniken Bergmannsheil, Ruhr-Universität Bochum, Germany

Abstract

Response inhibition processes are important for performance monitoring and are mediated via a network constituted by different cortical areas and basal ganglia nuclei. At the basal ganglia level, striatal GABAergic medium spiny neurons are known to be important for response selection, but the importance of the striatal GABAergic system for response inhibition processes remains elusive. Using a novel combination of behavioural, EEG and magnetic resonance spectroscopy (MRS) data we examine the relevance of the striatal GABAergic system for response inhibition processes. The study shows that striatal GABA levels modulate the efficacy of response inhibition processes. Higher striatal GABA levels were related to better response inhibition performance. We show that striatal GABA modulate specific subprocesses of response inhibition related to pre-motor inhibitory processes through the modulation of neuronal synchronization processes. To our knowledge this is the first study providing direct evidence for the relevance of the striatal GABAergic system for response inhibition functions and their cortical electrophysiological correlates in humans.

Keywords

striatum; GABA; response inhibition; EEG; magnetic resonance spectroscopy

[#]Address for correspondence C. Beste, Cognitive Neurophysiology, Department of Child and Adolescent Psychiatry, Faculty of Medicine of the TU Dresden, Germany, Schubertstrasse 42, D-01309 Dresden, Germany, Phone: +49-351-458-7072, Fax: +49-351-458-7318, christian.beste@uniklinikum-dresden.de.

Introduction

Response inhibition processes are important for cognitive control (for review: Bari & Robbins, 2013). Several lines of research using functional imaging in humans, clinical data as well as animal studies have shown that prefrontal cortical areas, like the dorsolateral prefrontal cortex (e.g. Hester et al., 2004), pre- and supplementary motor areas (pre-SMA, SMA) (e.g. Isoda & Hikosaka, 2007; Mostofsky et al., 2003; Simmonds et al., 2003), the inferior frontal cortex (e.g. Aron et al., 2004) and the anterior cingulate cortex (e.g. Rubia et al., 2001) are part of the response inhibition network. The response inhibition network also includes subcortical nuclei, which are hypothesized to receive stop commands from cortical structures used to incept or withhold a response (Duann et al., 2009). It has been shown that besides the subthalamic nucleus (e.g. Forstmann et al., 2012; van den Wildenberg et al., 2006), the striatum is important in response inhibition (e.g. Boehler et al., 2010; Beste et al., 2010). The striatum contains GABAergic medium spiny neurons (MSNs) (Bolam et al., 2000) that are regarded as the major computational element for action control processes in the basal ganglia (Humphries et al., 2010; Bar-Gad et al., 2003). The GABAergic MSNs are involved in the selection of different actions (Bar-Gad et al., 2003) and possibly also in the suppression of responses (Bari & Robbins, 2013). Yet, the striatum seem to be particular important for proactive as opposed to reactive inhibition (Aron, 2011).Given this putative MSN-mediated suppression of response options it is possible that striatal GABA levels largely determine the efficacy of response inhibition processes. Yet, the role of striatal GABAergic neural transmission in response inhibition remains elusive.

We investigate the role of the striatal GABA system for response inhibition combining data obtained from magnetic resonance spectroscopy (MRS) with EEG correlates of response inhibition. Using EEG data, different response inhibition subprocesses can be distinguished: (i) a frontal-midline N2 component closely related to theta oscillations reflecting pre-motor processes like conflict monitoring or updating of the response program; and (ii) a P3 component related to delta oscillations reflecting evaluative processing of the successful outcome of the inhibition (e.g. Huster et al., 2013; Beste et al., 2011; 2010). Beste et al. (2010) compared different basal ganglia diseases that differentially affect distinguishable basal ganglia subsystems. Using this comparative approach Beste et al. (2010) was able to show that especially the Nogo-N2 is affected by the nigro-striatal dopaminergic pathway, hence pointing to a role of striatal structures for cortical electrophysiological correlates of response inhibition. However, action selection in the striatum is largely determined by GABA is largely determined by GABA (Humphries et al., 2010). Recent results suggest that especially neural synchronization processes in striatal GABAergic medium spiny neurons are important for information encoding and behavioural control (Adler et al., 2013). It is therefore likely that striatal GABA levels strongly modulate response inhibition processes occurring in fronto-striatal networks. We hypothesize that higher striatal GABA levels come along with better performance in response inhibition; i.e. a lower rate of false alarms. False alarms are responses on Nogo stimulus, i.e., an error to withhold a response on Nogo stimuli. Striatal GABA concentrations largely determine striatal MSNs connectivity (Humphries et al., 2010) and it is the degree of connectivity in a neural assembly that is important for network synchronization (Kitano and Fukai, 2007). For the

electrophysiological processes we therefore hypothesize that the higher the striatal GABA level are correlated with the more synchronized electrophysiological oscillations in the delta or theta frequency bands and related response inhibition subprocesses.

Materials and Methods

Participants

The study sample consisted of forty right-handed healthy subjects (age 24.5 ± 5.9 years, range 20 – 30 years 10 females and 30 males) with no history of neurological or psychiatry disease and normal or corrected-to-normal vision. The study was approved by the Ethics committee of the Medical Faculty of the Ruhr-University Bochum, Germany.

Task

A standard Go/Nogo paradigm was used, similar to previous studies by our group (e.g. Ocklenburg et al., 2011; Beste et al., 2010). During the paradigm the words ‘PRESS’ and ‘STOP’ (translating to DRÜCK and STOPP in German) were presented on a computer screen. Upon presentation of the ‘PRESS’ stimulus, subjects were required to respond via a custom-made button as fast as possible (Go-stimulus). Upon presentation of the ‘STOPP’ stimulus, the subjects were required to withhold a response (Nogo-stimulus). Subjects were asked to respond within 400 ms on the ‘DRÜCK’ stimulus and refrain from responding on the ‘STOPP’ stimulus. Each trial lasted 1200ms. To increase time pressure in order to strengthen response tendencies in trials exceeding this time, a feedback stimulus (1000 Hz, 60 dB sound pressure level SPL) was given 1200 ms after the response, which was to be avoided by the subjects. The inter-trial interval (ITI) (time between two consecutive trials measured from the end of one trial to the beginning of the next trial) was jittered between 1200 and 1400 ms. The short period for reaction together with short ITI induced a strong response tendency and hence a high rate of false alarms.

EEG recording and analysis

The EEG was recorded from 65 Ag/AgCl electrodes using the extended 10/20 system (Pivik et al., 1993) against a reference electrode located on electrode position Cz. The sampling rate of all recordings was 1 kHz. Electrode impedances were kept below 5 kΩ. The EEG was digitally filtered off-line using an IIR filer with filter band-width between 0.5 and 20 Hz. Horizontal and vertical eye-movements were corrected in the EEG using independent component analysis (ICA) (infomax algorithm). Artifact rejection procedures were applied twice: automatically, with an amplitude threshold of ±80 μV, and visually by rejecting all trials contaminated by technical artifacts. Before quantifying event-related potentials (ERPs), the current source density (CSD) of the signals was calculated to achieve a reference-free evaluation (Nunez et al., 1997 and Perrin et al., 1989) using the following parameters: order of splines (m = 4), and the maximum degree of the Legendre polynomials (n = 10), with a precision of 2.72^{-7}. The data were segmented into 4096 ms long epochs. These long epochs were segmented to allow a reliable estimation of slow-oscillating frequencies in subsequent calculations of the phase-locking factor (PLF) (e.g. Beste et al., 2012; Beste et al., 2011). Time point zero denoting the time point of Go and Nogo-stimulus delivery was placed in the middle. With this epoch length a reliable quantification of slow

oscillations (delta and theta frequencies) is possible. For the time domain analysis, baseline correction was applied in the interval ranging from -200 ms to stimulus presentation. For the time-frequency analysis, the baseline was set between -600 and -400 ms before stimulus presentation.

On trials denoting response inhibition the Nogo-N2 was defined as the most negative deflection within the range of 150 to 300 ms after stimulus onset. The Nogo-P3 was defined as the most positive deflection from 320 till 500 ms. Amplitudes of the Go-N2 and Go-P3 were measured at the corresponding time point, where the Nogo component reached its maximum (Beste et al., 2010). The potentials were quantified at electrode FCz. As can be seen in the scalp topography plots on the Nogo-N2 and Nogo-P3 in Figure 3 the negativity for the Nogo-N2 is centered around electrode FCz and also the positivity of the Nogo-P3 is seen at this electrode site. The topography map on the phase-locking factor (PLF), which gives an estimate of neural synchronization processes also show that electrode FCz is the important electrode to analyze.

The PLF gives an estimate of the reliability of neural synchronization processes in time and frequency across trials (PLF; Roach & Mathalon, 2008; Tallon-Baudry et al., 2001). The PLF is independent of the signal's amplitude (Kolev and Yordanova, 1997) and varies between 0 and 1, with a value of 1 indicating perfect phase-locking across trials (i.e., high reliability of neural synchronization processes in time and frequency across trials). To obtain the PLF we first ran a time-frequency analysis using complex Morlet wavelets. These wavelets *w* can be generated in the time domain for different frequencies, *f*, according to the equation:

$$w(t,f)=A\exp(-t^2/2\sigma_t^2)\exp(2i\pi ft),$$

where *t* is time, $A=(\sigma_t\sqrt{\pi})^{-1/2}$, σ_t is the wavelet duration, and $i=\sqrt{-1}$. For analysis and TF-plots, a ratio of $f_0/\sigma_f = 5.5$ was used, where f_0 is the central frequency and σ_f is the width of the Gaussian shape in the frequency domain. The analysis was performed in the frequency range 0.1–20 Hz with a central frequency at 0.5 Hz intervals. For different f_0, time and frequency resolutions can be calculated as 2 σ_t and 2 σ_f, respectively. σ_t and σ_f are related by the equation $\sigma_t = 1/(2\pi\sigma_f)$. For each trial, the time-varying power in a given frequency band was calculated, which was obtained by squaring the absolute value of the convolution of the signal with the complex wavelet. The EEG data were collected outside the scanner in a different session. This was done to avoid the scanner artifacts that could impose problems in the analysis of the EEG data, especially when it comes to the time-frequency decomposition and the quantification of the phase-locking factor.

MRS data acquisition and analysis

MRS data was acquired on a 3 T Philips Achieva whole-body scanner using a 32-channel head coil. Fast T2-weighted images were obtained in axial, coronal and sagittal planes to enable placement of a 30×30×25 mm^3 MRS volume of interest (VOI) centered on the striatum. MRS spectra were acquired from VOIs placed in the left as well as the right striatum to rule out any laterality effects. MEGA-PRESS edited GABA spectra (Edden and

Barker, 2007; Mescher et al., 1998) were acquired from each VOI using the following parameters: repetition time (TR) = 2 s, echo time (TE) = 68 ms; a 15-ms editing pulse was applied either at 1.9 ppm (ON) or at 7.46 ppm (OFF); Segments of 16 ON and 16 OFF acquisitions of 2048 data points each and a spectral bandwidth of 2 kHz were interleaved 16 times, resulting in a total of 16x16=256 averages per MEGA-PRESS scan; total acquisition time = 8.5 min. A total of 16 additional averages without water suppression were acquired, one at the beginning of each of the ON and OFF scan segments, and used as reference data for frequency and phase correction. LCModel (Provencher et al., 1993) (version 6.2-0R), which fits *in vivo* MR spectra as a linear combination of single metabolite "basis spectra", was used for quantification (for details see suppl. material of Dydak et al., 2011). In particular, GABA was quantified from the MEGA-PRESS difference spectra using basis spectra created using density matrix simulations. Instead of using the in-built simplified GABA-fitting routine, we optimized the LCModel fitting parameters to allow the confounding macromolecule peak at 3.0 ppm to be largely fit by the flexible baseline function of LCModel (Dydak et al., 2011). While this additional degree of freedom results in slightly larger %SDs, it provides a more accurate estimation for pure GABA (Murdoch and Dydak 2011, Long et al. 2011, Dydak et al. 2011). All spectra had a linewidth of ≤10 Hz as determined by LCModel. All metabolite concentrations were computed as ratios to total creatine (tCr). The value of tCr for computing GABA/tCr was obtained from fitting the edit OFF spectrum of the MEGA-PRESS acquisition.

The fraction of gray matter (GM), white matter (WM) and cerebrospinal fluid (CSF) were calculated by superimposing the coordinates of the spectroscopy VOI on the high resolution T1-weighted images using the partial volume correction tool provided by N. Goulden and P. Mullins (http://biu.bangor.ac.uk/projects.php.en). The corresponding volume in the T1-weighted data set was then segmented into GM, WM and CSF fractions using the VBM8 toolbox (http://dbm.neuro.uni-jena.de/vbm/) as part of SPM8.

In addition to MEGA-PRESS spectra, regular short echo time Point REesolved Spectroscopy (PRESS) spectra (TR = 2 s, TE = 30 ms, 32 averages) were also obtained from the same VOIs and used for quantification of major metabolites including N-acetyl aspartate (NAA), total choline (tCho), tCr, myo-inositol (mI), and glutamate+glutamine (Glx). PRESS metabolite fits with a percentage standard deviation (%SD) value from LCModel over 20% were excluded from further analysis. For MEGA-PRESS, the corresponding %SD threshold was chosen to be 25% due to the flexible baseline approach. This threshold lies well within accepted standards used in GABA-MRS studies (e.g. Marjanska et al., 2013, Chowdhury et al., 2013, Silveri et al., 2013). However, the average %SD value for the GABA LCModel fits was 15.7 ± 3.5, and no GABA-edited spectra had to be excluded because of poor quality. A representative striatal GABA spectrum is displayed in Figure 1. Since no statistically significant differences were found within metabolite ratios between sides, prior to the regression analyses, the concentrations of different metabolites in the left and the right striatum were averaged across the left and right VOI for each subject (refer Figure 1).

The MRS data was collected prior to the conduction of the response inhibition experiment using EEG. Hence, MRS data does not reflect possible differential GABA levels for experimental trials in which response inhibition was successful and where response

inhibition was not successful. The GABA levels taken for the analysis reflect the general GABA level in the striatum; i.e., GABA levels were not determined in an event-related fashion for correct and incorrect Nogo-trials separately. This is because a reliable estimation of GABA concentrations requires several acquisition of the same volume. These several acquisitions cannot be performed in the time a single trial lasts. MRS data was integrated with the behavioural data and EEG data using linear regression analyses; i.e., we used the striatal GABA/tCr ratio as an independent variable to predict the degree of phase-locking and the amplitude values of the Nogo-N2 and Nogo-P3 signals. All significances for the correlations calculated were corrected using Bonferroni-Holm correction. The results presented are therefore controlled for possible type I errors.

Results

For descriptive statistics the mean and standard error of the mean (SEM) are given. For the left striatal VOI the GABA/tCr ratio was 0.224 ± 0.01 (SD = 0.05) and for the right striatal VOI 0.220 ± 0.01 (SD = 0.04) (GABA/tCr averaged over left and right striatal VOI was 0.221 ± 0.01 (SD = 0.03). Assuming a grey matter creatine concentration of 6 mM (Pouwels and Frahm, 1998) allows for an estimate of the striatal GABA concentration of 1.34 ± 0.03 mM, which is well in line with values reported for grey matter in general (Boer et al., 2011; Choi et al. 2006) and a thalamic volume of interest (Dydak et al. 2011).

For the behavioural data the rate of false alarms (i.e., percentage of Nogo trials on which a response occurred) in the Nogo condition was the main dependent variable of interest. The rate of false alarms was 13.87 ± 1.15. The regression analysis revealed a substantial inverse correlation ($r = -.541$; $R^2 = .292$; $p < .001$) between averaged striatal GABA/tCr level and the rate of false alarms (refer Figure 2). There were no such correlations when using reaction times on Go and Nogo-trials as well as reaction time slowing after the inhibition of responses (all $r < .2$; $p > .4$).

The event-related potentials on Go and Nogo trials are shown in Figure 3 at electrode FCz. The N2 amplitudes differed between Go (−13.15 ± 1.35) and Nogo trials (−21.16 ± 2.08) ($t_{39} = 6.37$; $p < .001$). The same was evident for the P3, where the P3 was smaller on Go (10.92 ± 1.68), than on Nogo trials (30.19 ± 2.69) ($t_{39} = -8.49$; $p < .001$). The regression analyses revealed that neither the Nogo-N2 amplitude nor the Nogo-P3 amplitude were correlated with averaged striatal GABA/tCr levels (all $r < .15$; $p > .4$) (refer Figure 2D). Similarly, there was also no correlation for the Go amplitudes (all $r < .2$; $p > .4$; not scatterplots shown). However, since especially neuronal synchronization processes in striatal GABAergic MSNs are important for information encoding and behavioural control (Adler et al., 2013) we repeated the regression analyses after the calculation of the phase-locking factor (PLF). The PLF is independent of the amplitude of the EEG signal (e.g. Kolev and Yordanova, 1997) and therefore provides information about the neuronal synchronization processes that are unrelated to the above analysis of ERP amplitudes. Figure 4 shows the mean PLF on Nogo trials.

As can be seen in Figure 4A the PLF was highest in the theta frequency band around a frequency of 5 Hz, which agrees with literature (for review: Huster et al., 2013). The mean

PLF was 0.57 ± .02. The regression analysis using the averaged striatal GABA/tCr level revealed a strong positive correlation with the PLF ($r = .612$; $R^2 = .374$ $p < .001$) as shown in Figure 4 in the Nogo-N2 time range. No correlation between averaged striatal GABA/tCr was evident in the Nogo-P3 time range at the 5Hz frequency ($r = .142$; $p > .5$) as well as other frequencies (all $r < .12$; $p > .6$). To test whether the gray matter fraction (GM%) of the MRS VOIs confounds the correlation between GABA/tCr and the response inhibition measures, we included the fraction of gray matter (GM%) (0.34 ± 0.006), white matter (WM %) (0.58 ± 0.005) and cerebrospinal fluid (CSF%) (0.07 ± 0.004) as additional predictors to GABA/tCr in the regression analyses. This regression model also revealed a predictive effect of averaged GABA/tCr for the rate of false alarms ($\beta = .541$; $t = 3.87$; $p < .001$), while neither GM%, WM% nor CSF% explained the variance (all $\beta < .042$; $t < -0.39$; $p > .9$) (overall model: $F(1,38) = 14.95$; $p < .001$). The same was the case for PLF in the Nogo-N2 range: There was a predictive effect of GABA/tCr ($\beta = .612$; $t = 5.85$; $p < .001$), but no effect of GM%, WM% and CSF% (all $\beta < .141$; $t < 1.21$; $p > .2$) (overall model: $F(1,38) = 34.27$; $p < .001$).

Using the levels of metabolites obtained from the PRESS spectra (i.e., NAA, tCho, tCr, mI and Glx) there were generally no significant correlations with behavioural and neurophysiological parameters of response inhibition (all $r < .3$; $p > .2$). The total (induced) wavelet power on Go and Nogo trials at electrode FCz are shown in Figure 4B and C. Using the total wavelet power, there we no correlations with the striatal GABA/tCr levels or any other metabolite obtained from the PRESS spectra (all $r < .15$; $p > .3$). This again underlines the specificity of effects regarding the obtained associations with the synchronization parameter.

Discussion

In the current study we examined the relevance of striatal GABA levels for response inhibition processes. Striatal GABA levels were measured using MRS. While the data quality and variability of our MRS data lies well within the normal reported ranges for other brain regions, it should be noted that this is the first study reporting GABA MRS data acquired from the striatum, which is a particularly challenging brain area to achieve high quality MRS data from. Thus a direct comparison to other literature values, validating the interpretation of our results, is not available. Response inhibition processes were examined using a standard Go/Nogo paradigm in combination with EEG data that was integrated with the MRS data. The results show that striatal GABA levels were predictive for response inhibition performance; i.e., higher striatal GABA levels were related to a lower rate of false alarms in the Nogo condition and hence better response inhibition performance. The results are unbiased with respect to the fraction of GM, WM and CSF in the voxel. Other metabolites using the PRESS spectra (i.e., NAA, tCho, tCr, mI and Glx) did not predict parameters of response inhibition performance underlining the specificity of the results obtained for the GABA levels.

The results provide evidence for the assumption that the striatal GABAergic system, known to be involved in the selection of different actions through GABAergic neural transmission (Bar-Gad et al., 2003), is also involved in the suppression of responses. Previous studies in

neurodegenerative disorders (e.g. Beste et al., 2010) were not able to show a role of the GABAergic system unequivocally, since GABAergic alterations were confounded with alterations in the dopaminergic system, which is of known importance for response inhibition processes (for review: Bari & Robbins, 2013).

While Silveri et al. (2013) have previously shown that higher GABA levels in the anterior cingulate cortex are related to better response inhibition, our results show that this also true for striatal structures. In this regard the results of our study are also in line with recent findings by Caprioli et al., (2014) who demonstrated that reductions in glutamate decarboxylase in rats are related to impulsive behaviour. However, our results reveal three important aspects:

First, EEG measures are usually considered to as being sensitive only to cortical processes, but not sensitive to subcortical basal ganglia processes. The current results show that a large amount of variance in EEG data is explained by neurobiochemical parameters of the basal ganglia, suggesting that EEG measures are sensitive to ‘remote’ basal ganglia processes. This is underlined by studies in basal ganglia diseases showing that pathophysiological processes affecting the basal ganglia modulate cortical electrophysiological correlates of cognitive control and inhibition processes recorded using the EEG (e.g. Beste and Saft, 2014; Beste et al., 2012; 2011; 2009). Possibly this effect arises as a consequence of the close functional and structural neuroanatomical connection between the prefrontal cortex and the basal ganglia (e.g. Chudasama and Robbins, 2006). Regarding the EEG data, striatal GABA levels were predictive for the PLF in the Nogo-N2 time window, but not in the Nogo-P3 time window. For the amplitudes of the Nogo-N2 and Nogo-P3 striatal GABA levels were not predictive.

Second, the striatal GABA system modulates the reliability of neural synchronization processes as reflected by the PLF and not the intensity of an electrophysiological process. As the strength of striatal MSN interconnectivity is largely determined by GABA (Humphries et al., 2010) and the degree of connectivity is known to determine network synchronization (e.g. Kitano and Fukai, 2007) as a major requirement for information encoding and behavioural control in the basal ganglia (Adler et al., 2013) it seems plausible that striatal GABA levels strongly modulate an electrophysiological measure of such neural synchronization processes. The importance of neural synchronization processes for response inhibition has also been shown by other electrophysiological studies (e.g. Beste et al., 2012; Swann et al., 2011). However, since the data structure obtained is necessarily correlative, it is also possible that altered neural synchronization processes at the cortical level may impact striatal GABA levels. Yet, in both cases the results stress the importance of the striatal GABAergic system for response inhibition. It is possible that GABA levels fluctuate between correct and incorrect Nogo trials, however, with current MRS methods it is not possible to measure GABA-levels in an event-related fashion.

Third, the results show that the striatal GABA system is only predictive for circumscribed electrophysiological subprocesses of response inhibition. It seems that striatal GABA levels modulate mechanisms reflecting pre-motor processes like conflict monitoring or updating of the response program (N2-related processes), but not mechanisms reflecting evaluative

processing of the successful outcome of the inhibition (P3-related processes) (e.g. Huster et al., 2013; Beste et al., 2011; 2010). The Nogo-N2 is more related to the motor aspects of response inhibition than is the case for the Nogo-P3 (e.g. Huster et al., 2013). Since the striatum plays a particularly important role in motor control and in the canceling and restraining of responses (Bari & Robbins, 2013; Bar-Gad et al., 2003), processes closely related to motor aspects of inhibition are more likely to be affected by GABA as a major basal ganglia neurotransmitter than processes related to subsequent evaluative processes.

The current study underlines the relevance of the GABAergic system for response inhibition processes. Besides these processes, other executive control functions like task switching, error monitoring and conflict processing have been shown to be modulated by striatal processes (Beste et al., 2014; van Schouwenburg et al., 2013; Willemssen et al., 2011; 2009). It is therefore conceivable that psychophysiological correlates of these functions may also show modulations by the striatal GABAergic system.

A limitation of the study is that the menstrual cycle of the female participants and hence levels of steroid hormones which have a known impact on GABA levels (Harada et al., 2011; Epperson et al., 2006) was not controlled for. Due to the low number of females in the present study it was also not possible to run reliable regression analyses using the factor ‘sex’ as predictor in the regression models. A further limitation of the study may be the lack of a control region used for GABA measurements that may be useful to determine the specificity of effects obtained in this study. It should also be kept in mind that the estimated average tissue GABA concentration is the sum of metabolic GABA located in the cell body, within the synaptic cleft, coupled to GABA-receptors and at extrasynaptic sites (Rae, 2014). It is therefore unclear whether this metric is better considered to be a determinant of the strength of GABAergic inhibition or a reflection of net inhibitory activity. In the striatum GABAergic interneurons represent only a small fraction of the cell population (and therefore a small fraction of tissue volume) but appear to contain much higher concentrations of GABA than projection neurons, so it is not clear what striatal GABAergic neurons (overview: Tepper and Bolam, 2004) mainly drive the effects.

In summary, the study shows, using a novel combination of MRS data and time-frequency decomposed EEG data, that striatal GABA levels predict efficacy of response inhibition processes. To our knowledge this is the first study providing direct evidence for the relevance of the striatal GABAergic system for response inhibition functions and their cortical electrophysiological correlates in humans. Using EEG methods we show that striatal GABA seems to affect only specific subprocesses of response inhibition that are related to pre-motor inhibitory processes through the modulation of the reliability of neural synchronization processes.

Acknowledgments

This work was supported by a Grant from the Deutsche Forschungsgemeinschaft (DFG) BE4045/10-1 and 10-2, as well as by NIH R01ES020529. We thank Dr. Richard Edden for providing the GABA-editing MRS sequence.

Literature

Adler A, Finkes I, Katabi S, Prut Y, Bergman H. Encoding by synchronization in the primate striatum. J Neurosci. 2013; 33:4854–4866. [PubMed: 23486956]

Aron AR. From reactive to proactive and selective control: developing a richer model for stopping inappropriate responses. Biol Psychiatry. 2011; 69:e55–68. [PubMed: 20932513]

Aron AR, Robbins TW, Poldrack RA. Inhibition and the right inferior frontal cortex. Trends Cogn Sci. 2004; 8:170–177. [PubMed: 15050513]

Bar-Gad I, Morris G, Bergman H. Information processing, dimensionality reduction and reinforcement learning in the basal ganglia. Prog Neurobiol. 2003; 71:439–473. [PubMed: 15013228]

Bari A, Robbins TW. Inhibition and impulsivity: behavioural and neural basis of response control. Prog Neurobiol. 2013; 108:44–79. [PubMed: 23856628]

Beste C, Saft C. Benign hereditary chorea as an experimental model to investigate the role of medium spiny neurons for response adaptation. Neuropsychologia. 2014; 59:124–129. [PubMed: 24835591]

Beste C, Mückschel M, Elben S, Hartman CJ, McIntyre CC, Saft C, Vesper J, Schnitzler A, Wojtecki L. Behavioral and neurophysiological evidence for the enhancement of cognitive control under dorsal pallidal deep brain stimulation in Huntington's disease. Brain Struct Funct. 201410.1007/s00429-014-0805-x

Beste C, Ness V, Lukas C, Hoffmann R, Stüwe S, Falkenstein M, Saft C. Mechanisms mediating parallel action monitoring in fronto-striatal circuits. Neuroimage. 2012; 62:137–146. [PubMed: 22617828]

Beste C, Ness V, Falkenstein M, Saft C. On the role of fronto-striatal neural synchronization processes for response inhibition – evidence from ERP phase- synchronization analyses in pre-manifest Huntington's disease gene mutation carriers. Neuropsychologia. 2011; 49:3484–3493. [PubMed: 21906607]

Beste C, Willemssen R, Saft C, Falkenstein M. Response inhibition subprocesses and dopaminergic pathways: basal ganglia disease effects. Neuropsychologia. 2010; 48:366–373. [PubMed: 19782093]

Beste C, Dziobek I, Hielscher H, Willemssen R, Falkenstein M. Effects of stimulus-response compatibility on inhibitory processes in Parkinson's disease. Eur J Neurosci. 2009; 29:855–860. [PubMed: 19200076]

Boehler CN, Appelbaum LG, Krebs RM, Hopf JM, Woldorff MG. Pinning down response inhibition in the brain-conjunction analyses of the Stop-signal task. NeuroImage. 2010; 52:1621–1632. [PubMed: 20452445]

Boer VO, Siero JC, Hoogduin H, van Gorp JS, Luijten PR, Klomp DW. High-field MRS of the human brain at short TE and TR. NMR Biomed. 2011; 24:1081–8. [PubMed: 21308826]

Bolam JP, Hanley JJ, Booth PA, Bevan MD. Synaptic organization of the basal ganglia. J Anat. 2000; 196:527–542. [PubMed: 10923985]

Caprioli A, Sawiak SJ, Merlo E, Theobald DEH, Spoelder M, Jupp B, Voon V, Carpenter A, Everitt BJ, Robbins TW, Dalley JW. Gamma aminobutyric acidergic and neuronal structural markers in the nucleus accumbens core underlie trait-like impulsive behavior. Biol Psychiatry. 2014; 75:115–123. [PubMed: 23973096]

Choi IY, Lee SP, Merkle H, Shen J. In vivo detection of gray and white matter differences in GABA concentration in the human brain. Neuroimage. 2006; 33:85–93. [PubMed: 16884929]

Chowdhury FA, O'Gorman RL, Nashef L, Elwes RD, Edden RA, Murdoch JB, Barker GJ, Richardson MP. Investigation of glutamine and GABA levels in patients with idiopathic generalized epilepsy using MEGAPRESS. J Magn Reson Imaging. 201410.1002/jmri.24611

Duann JR, Ide JS, Luo X, Li CS. Functional connectivity delineates distinct roles of the inferior frontal cortex and presupplementary motor area in stop signal inhibition. J Neurosci. 2009; 29:10171–10179. [PubMed: 19675251]

Dydak U, Jiang YM, Long LL, Zhu H, Chen J, Li WM, Edden RA, Hu S, Fu X, Long Z, Mo XA, Meier D, Harezlak J, Aschner M, Murdoch JB, Zheng W. In vivo measurement of brain GABA concentrations by magnetic resonance spectroscopy in smelters occupationally exposed to manganese. Environ Health Perspect. 2011; 119:219–24. [PubMed: 20876035]

Edden RAE, Barker PB. Spatial effects in the detection of γ - aminobutyric acid: Im proved sensitivity at high fields using inner volume saturation. Magnc Reson Med. 2007; 58:1276–1282.

Epperson CN, Gueorguieva R, Czarkowski KA, Stiklus S, Sellers E, Krystal JH, Rothman DL, Mason GF. Preliminary evidence of reduced occipital concentrations in puerperal women: a 1H-MRS study. Psychopharmacology. 2006; 186:425–433. [PubMed: 16724188]

Forstmann BU, Keuken MC, Jahfari S, Bazin PL, Neumann J, Schäfer A, Anwander A, Turner R. Cortico-subthalamic white matter tract strength predicts interindividual efficacy in stopping a motor response. Neuroimage. 2012; 60:370–375. [PubMed: 22227131]

Harada M, Kubo H, Nose A, Nishitani H, Matsuda T. Measurement of variation in the human cerebral GABA level by in vivo MEGA-editing proton MR spectroscopy using a clinical 3 T instrument and its dependence on brain region and the female menstrual cycle. Hum Brain Mapp. 2011; 32:828–833. [PubMed: 20645307]

Hester RL, Murphy K, Foxe JJ, Foxe DM, Javitt CD, Garavan H. Predicting success: patterns of cortical activation and deactivation prior to response inhibition. J Cogn Neurosci. 2004; 16:776–785. [PubMed: 15200705]

Humphries MD, Wood R, Gurney K. Reconstructing the three-dimensional GABAergic microcircuit of the striatum. Plos Comp Biol. 2010; 6:e1001011.

Huster RJ, Enriquez-Geppert S, Lavallee CF, Falkenstein M, Herrmann CS. Electroencephalography or response inhibition tasks: functional networks and cognitive contributions. Int J Psychophysiol. 2013; 87:217–233. [PubMed: 22906815]

Isoda M, Hikosaka O. Switching from automatic to controlled action by monkey medial frontal cortex. Nat Neurosci. 2007; 10:240–248. [PubMed: 17237780]

Kitano K, Fukai T. Variability v.s. sychronicity of neuronal activity in local cortical network models with different wiring topologies. J Comput Neurosci. 2007; 23:237–250. [PubMed: 17415629]

Kolev V, Yordanova J. Analysis of phase-locking is informative for studying event-related EEG activity. Biol Cybern. 1997; 76:229–235. [PubMed: 9151420]

Long Z, Murdoch JB, Xu J, Dydak U. GABA Fitting for MEGA-PRESS Sequences with Different Selective Inversion Frequencies. Proc Intl Soc Mag Reson Med. 2011; 19:1399.

Marjańska M, Lehéricy S, Valabrègue R, Popa T, Worbe Y, Russo M, Auerbach EJ, Grabli D, Bonnet C, Gallea C, Coudert M, Yahia-Cherif L, Vidailhet M, Meunier S. Brain dynamic neurochemical changes in dystonic patients: A magnetic resonance spectroscopy study. Mov Disord. 2013; 28:201–209. [PubMed: 23239076]

Mescher M, Merkle H, Kirsch J, Garwood M, Gruetter R. Simultaneous in vivo spectral editing and water suppression. NMR Biomed. 1998; 11:266–272. [PubMed: 9802468]

Mostofsky SH, Schafer JG, Adrams MT, Goldberg MC, Flower AA, Boyce A, Courtney SM, Calhoun VD, Kraut MA, Denckla MB, Pekar JJ. fMRI evidence that the neural basis of response inhibition is task-dependent. Brain Res Cogn Brain Res. 2003; 17:419–430. [PubMed: 12880912]

Murdoch JB, Dydak U. Modeling MEGA-PRESS macromolecules for a better grasp of GABA. Proc Intl Soc Mag Reson Med. 2011; 19:1394.

Nunez PL, Srinivasan R, Westdorp AF, Wijesinghe RS, Tucker DM, Silberstein RB, Cadusch PJ. EEG coherency. I: Statistics, reference electrode, volume conduction, Laplacians, cortical imaging, and interpretation at multiple scales. Electroencephalogr Clin Neurophysiol. 1997; 103:499–515. [PubMed: 9402881]

Ocklenburg S, Güntürkün O, Beste C. Lateralized neural mechanisms underlying the modulation of response inhibition processes. Neuroimage. 2011; 55:1771–1778. [PubMed: 21256235]

Perrin F, Pernier J, Bertrand O, Echallier JF. Spherical splines for scalp potential and current densitiy mapping. Eletroencephalogr Clin Neurophysiol. 1989; 72:184–187.

Pivik RT, Broughton RJ, Coppola R, Davidson RJ, Fox N, Nuwer MR. Guidelines for the recording and quantitative analysis of electroencephalographic activity in research contexts. Psychophysiology. 1993; 30:547–558. [PubMed: 8248447]

Pouwels PW, Frahm J. Regional Metabolite Concentrations in Human Brain as Determined by Quantitative Localized Proton MRS. Magn Reson Med. 1998; 39:53–60. [PubMed: 9438437]

Provencher SW. Estimation of metabolite concentrations from localized in vivo proton NMR spectra. Magn Reson Med. 1993; 30:672–679. [PubMed: 8139448]

Rae CD. A guide to the metabolic pathways and function of metabolites observed in human brain (1)h magnetic resonance spectra. Neurochem Res. 2014; 39:1–36. [PubMed: 24258018]

Roach BJ, Mathalon DH. Event-related EEG time-freqeuncy analysis: an overview of measures and an analysis of early gamma band phase locking in schizophrenia. Schizophr Bull. 2008; 34:907–926. [PubMed: 18684772]

Rubia K, Russel T, Overmeyer S, Brammer MJ, Bullmore ET, Sharma T, Simmons A, Williams SC, Giampietro V, Andrew CM, Taylor E. Mapping motor inhibition: conjunctive brain activations across different version of go/no-go and stop tasks. Neuroimage. 2001; 13:250–261. [PubMed: 11162266]

Silveri MM, Sneider JT, Crowley DJ, Covell MJ, Acharya D, Rosso IM, Jensen JE. Frontal lobe γ -aminobutyric acid levels during adolescence: associations with impulsivity and response inhibition. Biol Psychiatry. 2013; 74:296–304. [PubMed: 23498139]

Swann N, Poizner H, Houser M, Gould S, Greenhouse I, Cai W, Strunk J, George J, Aron AR. Deep brain stimulation of the subthalamic nucleus alters the cortical profile of response inhibition in the beta frequency band: a scalp EEG study in Parkinson's disease. J Neurosci. 2011; 31:5721–5729. [PubMed: 21490213]

Tallon-Baudry C, Bertrand O, Fischer C. Oscillatory synchrony between human extrastriate areas during visual short-term memory maintenance. J Neurosci. 2001; 21:RC177. [PubMed: 11588207]

Tepper JM, Bolam JP. Functional diversity and specificity of neostriatal interneurons. Curr Opin Neurobiol. 2004; 14:685–692. [PubMed: 15582369]

van den Wildenberg WP, van Boxtel GJ, van der Molen MW, Bosch DA, Speelman JD, Brunia CH. Stimulation of the subthalamic region facilitates the selection and inhibition of motor responses in Parkinson's disease. J Cogn Neurosci. 2006; 18:626–636. [PubMed: 16768365]

Van Schouwenburg MR, den Ouden HE, Cools R. Selective attentional enhancement and inhibition of fronto-posterior connectivity by the basal ganglia during attention switching. Cereb Cortex. 2013 [Epub ahead of print].

Willemssen R, Falkenstein M, Schwarz M, Müller T, Beste C. Effects of aging, Parkinson's disease, and dopaminergic medication on response selection and control. Neurobiol Aging. 2011; 32:327–335. [PubMed: 19269061]

Willemssen R, Müller T, Schwarz M, Falkenstein M, Beste C. Response monitoring in de novo patients with Parkinson's disease. PloS One. 2009:e4898. [PubMed: 19325909]

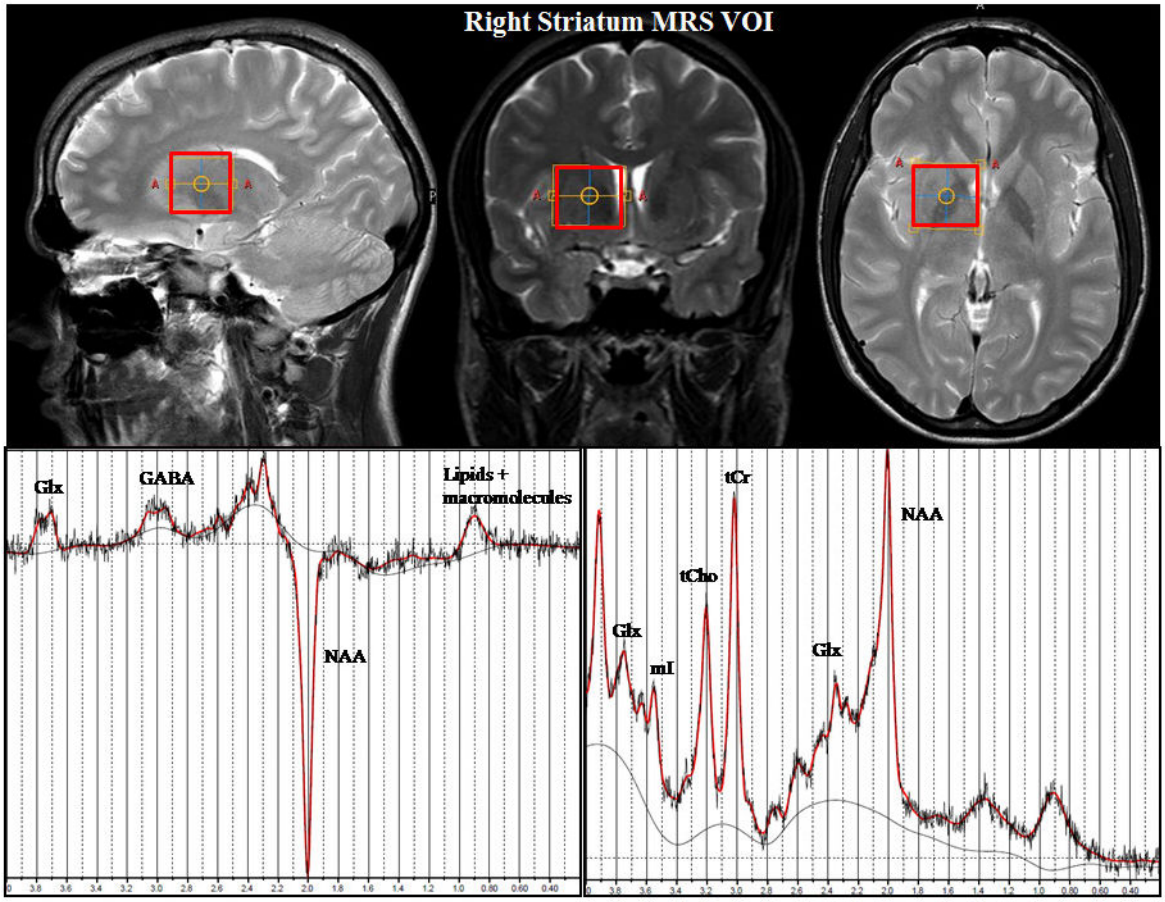

Figure 1.

Representative MRS VOI placement in the right striatum (top) and the LCModel fits of MEGA-PRESS GABA spectrum (bottom left) and short TE PRESS spectrum (bottom right) acquired from the VOI.

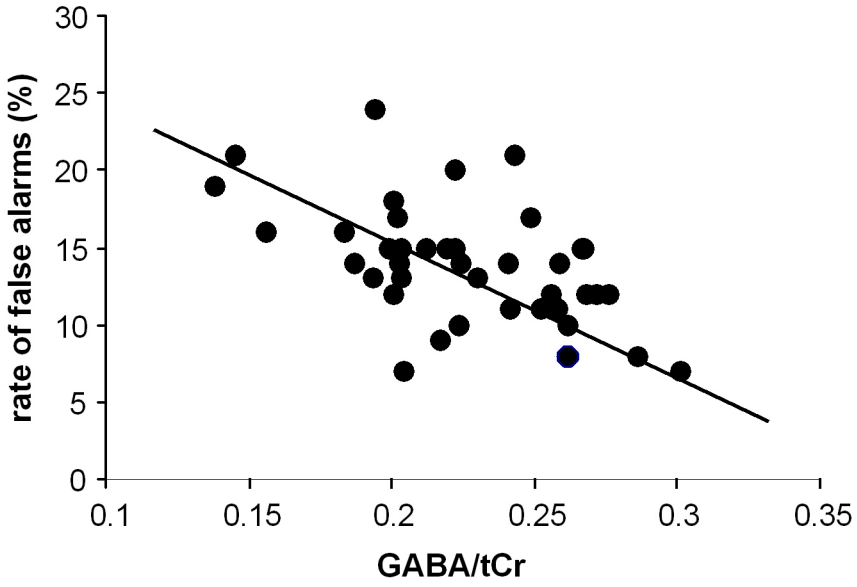

Figure 2.
Scatterplot denoting the correlation between striatal GABA levels and the rate of false alarms in the Nogo condition.

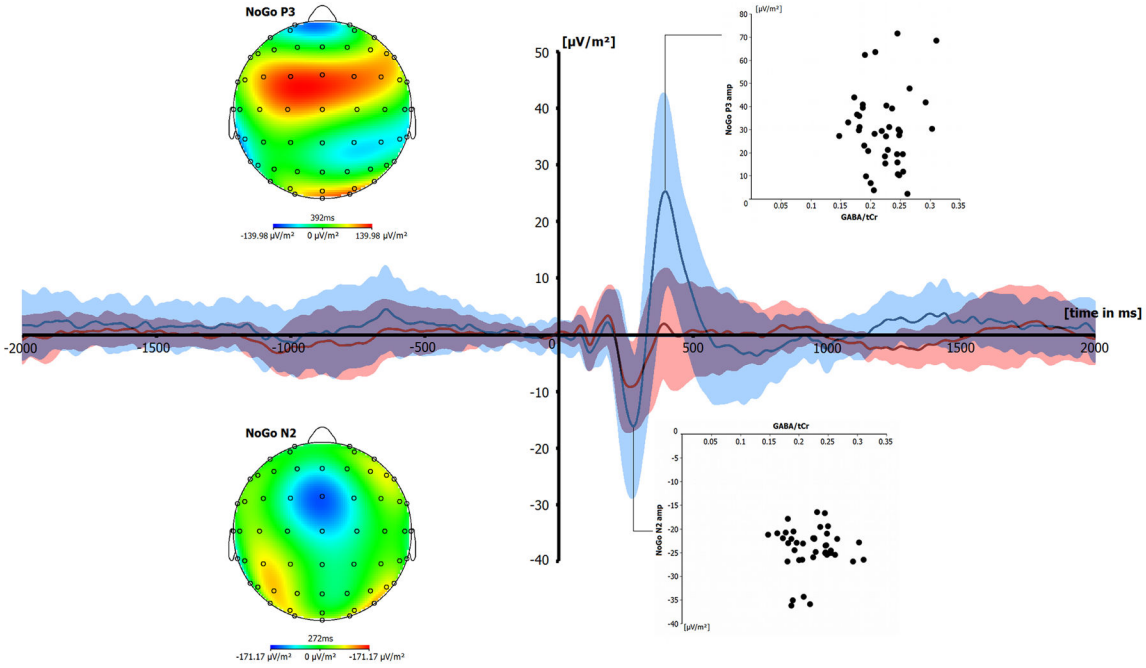

Figure 3.

Grand average plot of Go and Nogo ERPs at electrode FCz. Time point zero denotes the time point of Go and Nogo stimulus presentation. The scalp topography plots denote the topography of the Nogo-N2 and Nogo-P3 at their peak maximum. Red lines denote Go-trials and blue lines denote Nogo trials. Red and blue shadings denote the standard deviation at each time point. The scatterplots denote the interrelation between striatal GABA levels and the Nogo-N2 amplitudes and Nogo-P3 amplitudes.

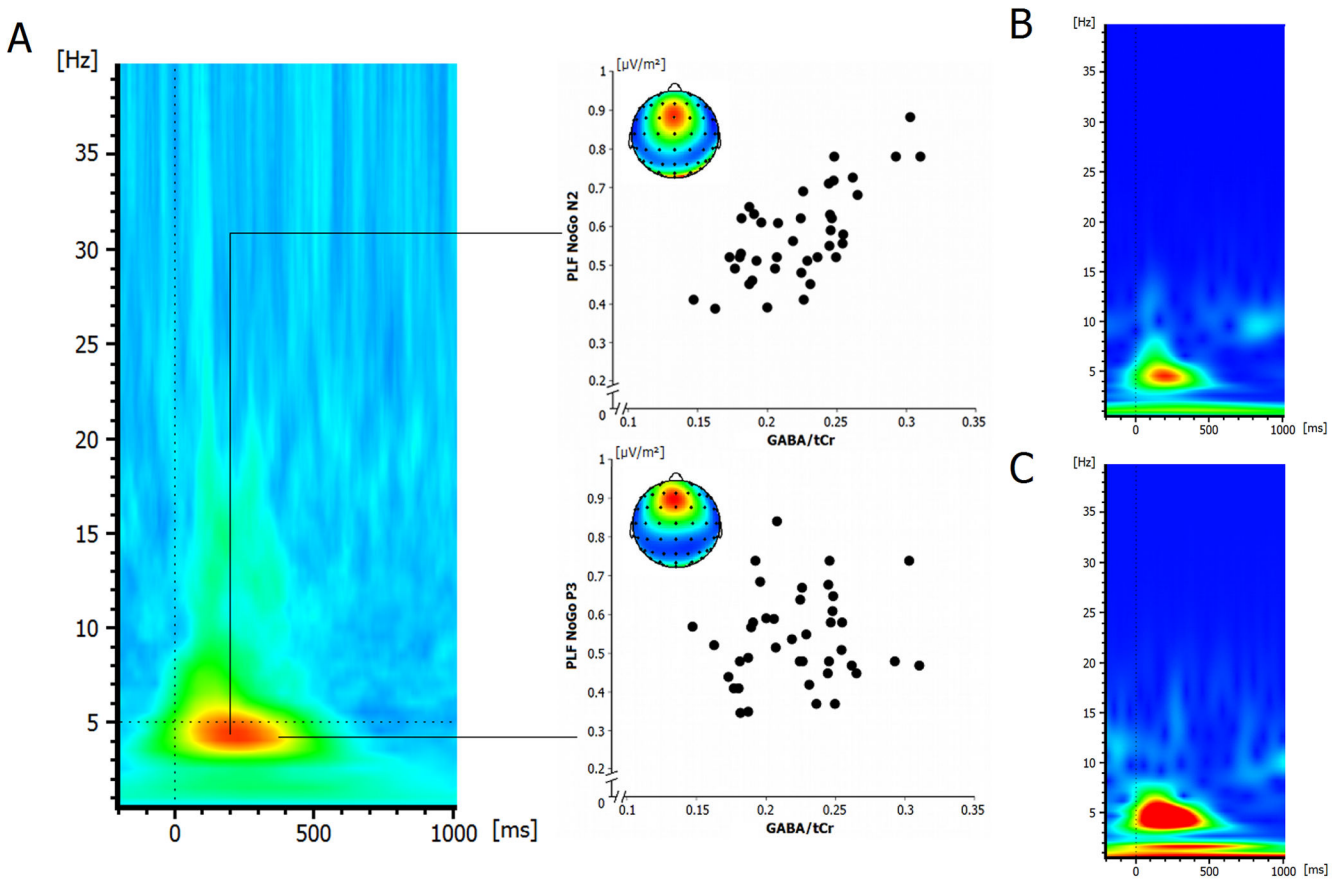

Figure 4.

(A) Grand average plot of the phase-locking factor (PLF) on Nogo trials at electrode FCz. Warm colors indicate high phase-locking, cold colors denotes low phase-locking. The scatterplots show the correlation between striatal GABA levels and the PLF in the Nogo-N2 time window and the Nogo-P3 time window. Black lines linking the scatter plot with the relative time point (region in the PL-plot) indicate the time point from which the PL for the N2 and the P3 component was extracted. Warm colours in the maps denote electrode sites where the phase-locking factor was high, cold colour denote electrode sites where the phase-locking factor was low. (B) Time frequency plot denoting the total (induced) wavelet power at electrode FCz for Go trials. (C) Time frequency plot denoting the total (induced) wavelet power at electrode FCz for Nogo trials.